Supporting Information

Eckel-Mahan et al. 10.1073/pnas.1118726109

SI Methods

Global Metabolic Profiling. Livers from age-matched, adult, male mice from WT and *Clock*$^{-/-}$ were used for liver isolation at zeitgeber (ZT)3, ZT9, ZT15, and ZT21, with ZT0 corresponding to lights on and ZT12 corresponding to lights off in the animal facility. Animals were housed in a 12-h light/12-h dark schedule. Livers were harvested, rinsed briefly in PBS, and immediately frozen in liquid nitrogen. Frozen liver samples were shipped to Metabolon. The metabolic profiling platform used for this kind of analysis by Metabolon combines three independent platforms: ultrahigh performance liquid chromatography/tandem mass spectrometry (UHPLC/MS/MS) optimized for basic species, UHPLC/MS/MS optimized for acidic species, and gas chromatography/mass spectrometry (GC/MS) (1). It was recently shown that this integrated platform enables the high-throughput collection and relative quantitative analysis of analytical data and identifies a large number and broad spectrum of molecules with a high degree of confidence (2). Briefly, a comparable amount of liver tissue from each replicate animal for WT and *Clock*$^{-/-}$ was used. Samples were processed essentially as described previously (2–4). Tissue was homogenized in a 5× volume of water (wt:vol) by the addition of grinding beads and shaking at the rate of 1,000 strokes per minute for 5 min using a GlennMills GenoGrinder 2000. A total of 100 μL of homogenate was withdrawn for subsequent analyses. Using an automated liquid handler (Hamilton LabStar), protein was precipitated from the homogenate with 450 μL of HPLC-grade methanol that contained four standards to report on extraction efficiency. Samples were shaken for 2 min then centrifuged for 5 min. The resulting supernatant was split into equal aliquots of 110 μL for analysis on the three platforms, with a fourth aliquot reserved for backup. Aliquots, dried under nitrogen and vacuum desiccated, were subsequently either reconstituted in 0.1% formic acid in water (100 μL, acidic conditions) or in 6.5 mM ammonium bicarbonate in water, pH 8 (100 μL, basic conditions) for the two UHPLC/MS/MS analyses or derivatized to a final volume of 50 μL for GC/MS analysis using equal parts bistrimethyl-silyl-trifluoroacetamide and solvent mixture acetonitrile:dichloromethane:cyclohexane (5:4:1) with 5% triethylamine (vol/vol) at 60 °C for 1 h. In addition, three types of controls were analyzed in concert with the experimental samples: samples generated from pooled experimental samples served as technical replicates throughout the dataset, extracted water samples served as process blanks, and a mixture of standards spiked into every analyzed sample allowed instrument performance monitoring. Experimental samples and controls were randomized across a 2-d platform run. For UHPLC/MS/MS analysis, aliquots were separated using a Waters Acquity UPLC (Waters) and analyzed using an LTQ mass spectrometer (Thermo Fisher Scientific), which consisted of an electrospray ionization source and linear ion-trap mass analyzer. The MS instrument scanned 99–1,000 *m/z* and alternated between MS and MS/MS scans using dynamic exclusion with ∼6 scans per second. Derivatized samples for GC/MS were separated on a 5% phenyldimethyl silicone column with helium as the carrier gas and a temperature ramp from 60 °C to 340 °C and then analyzed on a Thermo-Finnigan Trace DSQ MS (Thermo Fisher Scientific) operated at unit mass resolving power with electron impact ionization and a 50–750 atomic mass unit scan range. Metabolites were identified by automated comparison of the ion features in the experimental samples to a reference library of chemical standard entries that included retention time, molecular weight (*m/z*), preferred adducts, and in-source fragments as well as associated MS spectra and were curated by visual inspection for quality control using software developed at Metabolon (5).

CircadiOmics. We developed a computational framework that integrates the above-described liver metabolome data with the following sources of information: Kyoto Encyclopedia of Genes and Genomes (KEGG), Circa and GEO, BioGRID, IntAct and MINT, Bmal1 ChIP-seq, and MotifMap.

KEGG. KEGG (6–8) contains pathway information for metabolism and other cellular processes, manually curated from the literature. We were able to map 223 of the 309 named metabolites to known KEGG pathways using the KEGG application programming interface (8). For each metabolite, we extracted all of the enzymes associated with reactions where the metabolite appears as a substrate or a product.

Circa and GEO. Circa (9) and GEO (10) provide tissue-specific circadian gene expression profiles obtained from high-resolution DNA microarray experiments. Briefly, gene expression in liver cells was measured every hour for 48 h using microarrays. These data were downloaded from GEO (GSE13093) and the time lines were synchronized with the metabolome data to yield a complete 24-h cycle. The data were also used to carefully filter the list of genes used in the networks, retaining only genes that have significant expression levels in the relevant condition (mouse liver, WT, and thereby removing some protein–protein, transcription factor–enzyme, and enzyme–metabolite edges that may be spurious.

BioGRID, IntAct, and MINT. These databases (11–13) were used to extract the list of protein–protein interactions for the various enzymes and transcription factors.

Bmal1 ChIP-seq. Chromatin immunoprecipitation-based analysis along with bioinformatics and high-throughput DNA microarrays were used to generate a genome-wide expression profile for Bmal1 in the liver (14).

MotifMap. MotifMap (15, 16) is the most comprehensive database of putative regulatory transcription factor binding sites. The mouse transcription factor binding matrices come from two major sources, TRANSFAC (17) and Jaspar (10) and encompass over 800 binding matrices, corresponding to over 400 distinct transcription factors. Briefly, each position weight matrix is used to scan the mouse genome for potential binding sites. Every site is assigned the following three scores: (*i*) motif matching score (*Z* score); (*ii*) conservation score (Bayesian branch length score, BBLS), calculated using a multiple alignment of 30 genomes from mouse to zebrafish; and (*iii*) false discovery rate (FDR), obtained by shuffling the columns of the binding matrix and using Monte Carlo methods. We retained only those sites for which the *Z* score was greater than 4.0, BBLS was greater than or equal to 0.5, and FDR less than or equal to 0.1.

Preparation of cDNA and Quantitative Real-Time Reverse Transcription. RNA was isolated and cDNA prepared as previously described (18). The primers for ChIP, semiquantitative PCR, and real-time qPCR were obtained from refs. 18–22 or designed by Primer 3 (v. 0.4.0) and are as follows:

Upp2 F: GCACACTGCTGTGATGTT
Upp2 R: CTGCTACAGTTGAACAGA
Cs F: GATTGTGCCCAATGTCCTCT
Cs R: TTCATCTCCGTCATGCCATA
Upp2 F: ChIP: CTGCACTCAAACTTCCAGCA
Upp2 R: ChIP: TGAGGCCTCCTCAATTAACC
Dbp F ChIP: ACACCCGCATCCGGTAGC
Dbp R ChIP: CCACTTCGGGCCAATGAG.

Chromatin Immunoprecipitation. Chromatin immunoprecipitation was performed as described in ref. 23 with some modifications.

One hundred micrograms of frozen (previously unthawed after frozen) liver tissue was minced in PBS containing protease inhibitors. Minced tissue was crosslinked with DSG (2 mM final) in PBS containing MgCl (10 mM final) for 45 min at 25 °C. Formaldehyde (1% final) was added for additional crosslinking at 25 °C for 15 min. Samples were spun at low speed and resuspended in PBS with protease inhibitors for homogenization. Following homogenization, samples were spun at low speed and resuspended in 2 mL ChIP sonication buffer (1% Triton X-100, 50 mM Tris, pH 8.1, 5 mM EDTA, 0.1% deoxycholate, 150 mM NaCl) containing protease inhibitors. Following sonication, samples were spun at 16,000 × *g* in a microcentrifuge and supernatants were diluted 1:4 in ChIP dilution buffer (0.01% SDS, 1.1% Triton X-100, 1.2 mM EDTA, 16.7 mM Tris, pH 8.1, 167 mM NaCl), and immunoprecipitated with α-CLOCK antibody (Santa Cruz; sc-6927) or control IgG overnight. Protein:DNA complexes were captured with blocked protein G-agarose beads and following elution, reverse crosslinking, proteinase K digestion, extraction, and precipitation (as described in ref. 23), ChIP samples were diluted in 120 μL ddH_20. Six microliters of each ChIP sample was used for qPCR analysis by primers spanning E box containing regions in the *Upp2* and *Dbp* promoters (for primer sequences, see *Methods* for qPCR).

Statistical Analysis for Metabolite Profiling. Data from each experimental group were assessed through replicates ($n = 5$) for representative mean and image. For statistical analyses and data display purposes of the metabolomics data, any missing values were assumed to be below the limits of detection; these values were imputed with the compound minimum (minimum value imputation). The analysis for this paper was generated using Array Studio software. Array Studio, Array Viewer, and Array Server and all other Omicsoft products or service names are registered trademarks or trademarks of Omicsoft. *F* tests resulting from the two-way ANOVA were used to identify biochemicals that differed significantly between $Clock^{-/-}$ and wild-type groups at each time point; $P < 0.05$ was considered significant. Multiple comparisons were accounted for by estimating the false discovery rate using *q* values (24).

Permutation Tests. Additional statistical analysis of how circadian the different trajectories were involved choosing mice at random at each time point (for instance, an observation from mouse 1 for ZT3, mouse 3 for ZT9, mouse 2 for ZT15, and mouse 5 for ZT21). This can be done in $5^4 = 625$ possible ways (five mice to choose from at each of the four time points) for each metabolite. Generation of all 625 different trajectories for each metabolite in each condition was accomplished and the exact number of these trajectories that passed a *P* value of 0.05 in the JTK_Cycle software, and computed the permutation test score was counted: (permutation test score = number of circadian time trajectories using JTK_Cycle/total number of possible trajectories [= 625]. These results are now included in Dataset S4, under *Permutation Test*.)

1. Reitman ZJ, et al. (2011) Profiling the effects of isocitrate dehydrogenase 1 and 2 mutations on the cellular metabolome. *Proc Natl Acad Sci USA* 108:3270–3275.
2. Evans AM, DeHaven CD, Barrett T, Mitchell M, Milgram E (2009) Integrated, nontargeted ultrahigh performance liquid chromatography/electrospray ionization tandem mass spectrometry platform for the identification and relative quantification of the small-molecule complement of biological systems. *Anal Chem* 81:6656–6667.
3. Ohta T, et al. (2009) Untargeted metabolomic profiling as an evaluative tool of fenofibrate-induced toxicology in Fischer 344 male rats. *Toxicol Pathol* 37:521–535.
4. Ohta Y, Kobayashi Y, Konishi S, Hirano S (2009) Speciation analysis of selenium metabolites in urine and breath by HPLC- and GC-inductively coupled plasma-MS after administration of selenomethionine and methylselenocysteine to rats. *Chem Res Toxicol* 22:1795–1801.
5. Dehaven CD, Evans AM, Dai H, Lawton KA (2010) Organization of GC/MS and LC/MS metabolomics data into chemical libraries. *J Cheminform* 2:9.
6. Kanehisa M, Goto S (2000) KEGG: Kyoto encyclopedia of genes and genomes. *Nucleic Acids Res* 28:27–30.
7. Kanehisa M, Goto S, Furumichi M, Tanabe M, Hirakawa M (2010) KEGG for representation and analysis of molecular networks involving diseases and drugs. *Nucleic Acids Res* 38:D355–D360.
8. Kanehisa M, et al. (2006) From genomics to chemical genomics: New developments in KEGG. *Nucleic Acids Res* 34:D354–D357.
9. Hughes M, et al. (2007) High-resolution time course analysis of gene expression from pituitary. *Cold Spring Harb Symp Quant Biol* 72:381–386.
10. Sandelin A, Alkema W, Engström P, Wasserman WW, Lenhard B (2004) JASPAR: An open-access database for eukaryotic transcription factor binding profiles. *Nucleic Acids Res* 32:D91–D94.
11. Stark C, et al. (2006) BioGRID: A general repository for interaction datasets. *Nucleic Acids Res* 34(Database issue):D535–D539.
12. Aranda B, et al. (2010) The IntAct molecular interaction database in 2010. *Nucleic Acids Res* 38:D525–D531.
13. Ceol A, et al. (2009) MINT, the molecular interaction database: 2009 update. *Nucleic Acids Res* 38:D532–D539.
14. Hatanaka F, et al. (2010) Genome-wide profiling of the core clock protein BMAL1 targets reveals a strict relationship with metabolism. *Mol Cell Biol* 30:5636–5648.
15. Daily K, Patel VR, Rigor P, Xie X, Baldi P (2011) MotifMap: Integrative genome-wide maps of regulatory motif sites for model species. *BMC Bioinformatics* 12:495.
16. Xie X, Rigor P, Baldi P (2009) MotifMap: A human genome-wide map of candidate regulatory motif sites. *Bioinformatics* 25:167–174.
17. Matys V, et al. (2003) TRANSFAC: Transcriptional regulation, from patterns to profiles. *Nucleic Acids Res* 31:374–378.
18. Nakahata Y, et al. (2008) The NAD+-dependent deacetylase SIRT1 modulates CLOCK-mediated chromatin remodeling and circadian control. *Cell* 134:329–340.
19. Im YS, et al. (2009) Enhanced cytotoxicity of 5-FU by bFGF through up-regulation of uridine phosphorylase 1. *Mol Cell* 28:119–124.
20. Honda A, et al. (2010) Attenuation of cadmium-induced testicular injury in metallothionein-III null mice. *Life Sci* 87:545–550.
21. Pattyn F, Speleman F, De Paepe A, Vandesompele J (2003) RTPrimerDB: The real-time PCR primer and probe database. *Nucleic Acids Res* 31:122–123.
22. Ripperger JA, Schibler U (2006) Rhythmic CLOCK-BMAL1 binding to multiple E-box motifs drives circadian Dbp transcription and chromatin transitions. *Nat Genet* 38:369–374.
23. Hwang-Verslues WW, Sladek FM (2008) Nuclear receptor hepatocyte nuclear factor 4alpha1 competes with oncoprotein c-Myc for control of the p21/WAF1 promoter. *Mol Endocrinol* 22:78–90.
24. Storey JD, Tibshirani R (2003) Statistical significance for genomewide studies. *Proc Natl Acad Sci USA* 100:9440–9445.

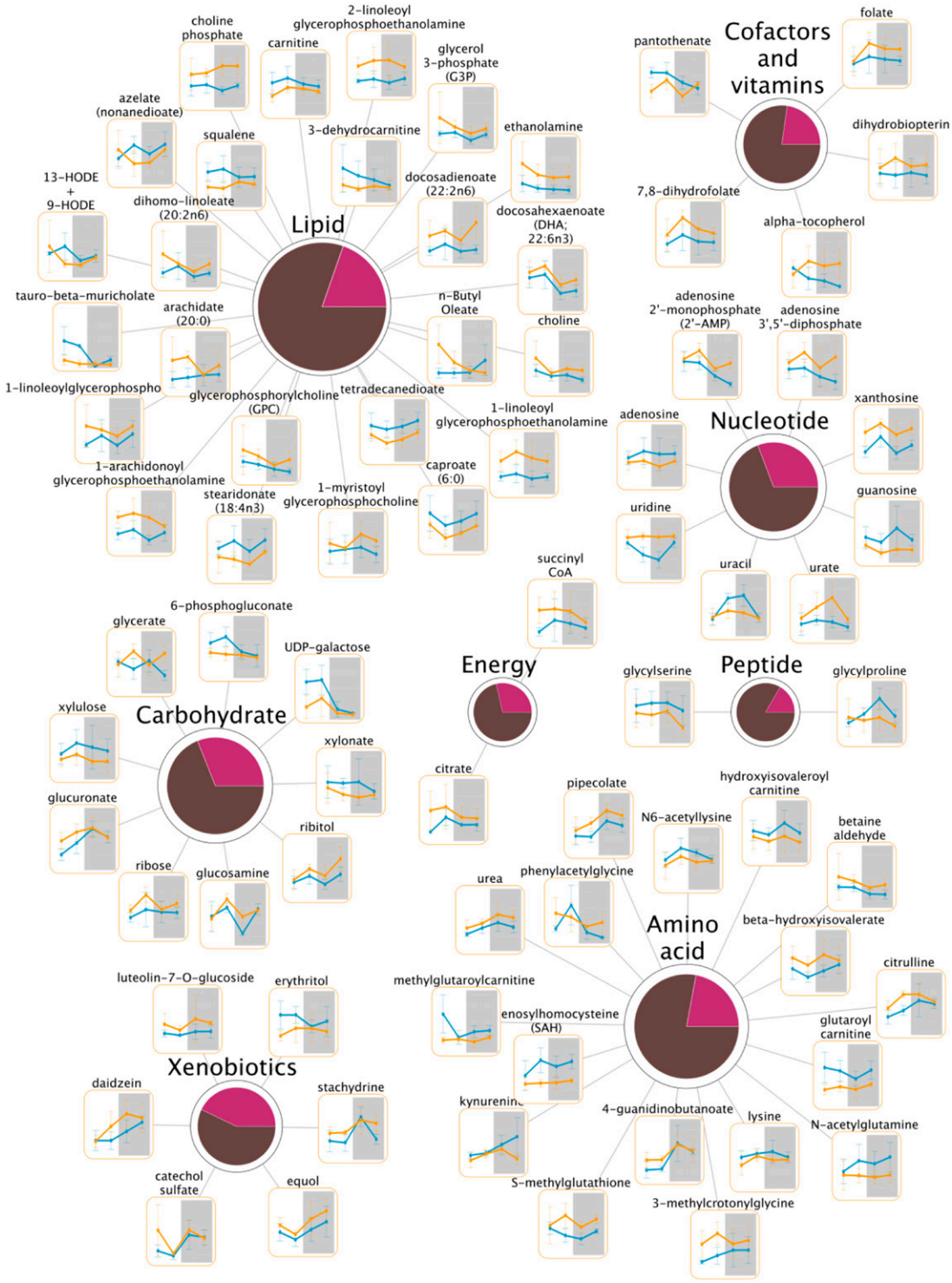

Fig. S1. Metabolites altered in *Clock*$^{-/-}$ livers. Metabolites altered in *Clock*-deficient livers are graphed around metabolic pathways. The pink shading within metabolic pathway centers depicts the percentage of named metabolites that were altered compared with WT livers. Brown shading depicts the percentage of metabolites within the metabolic pathway that were unchanged in *Clock*-deficient livers compared with WT livers.

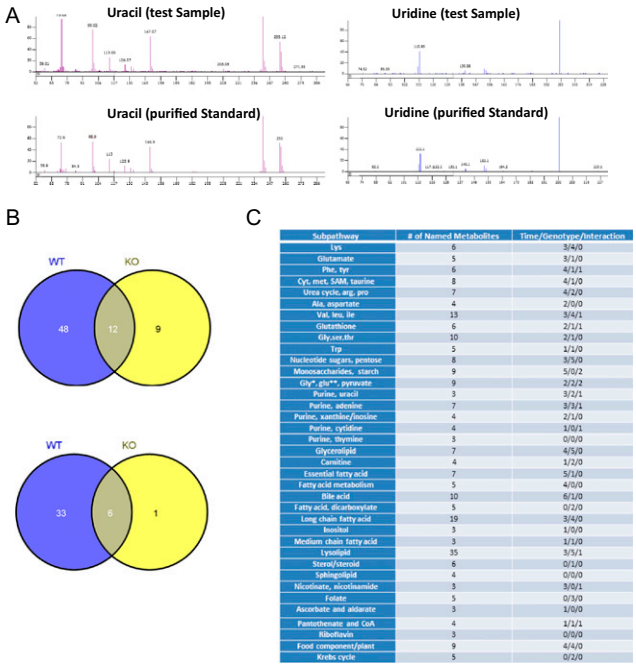

Subpathway	# of Named Metabolites	Time/Genotype/Interaction
Lys	6	3/4/0
Glutamate	5	3/1/0
Phe, tyr	6	4/1/1
Cys, met, SAM, taurine	8	4/1/0
Urea cycle, arg, pro	7	4/2/0
Ala, aspartate	4	2/0/0
Val, leu, ile	13	3/4/1
Glutathione	6	2/1/1
Gly,ser,thr	10	2/1/0
Trp	5	1/1/0
Nucleotide sugars, pentose	8	3/5/0
Monosaccharides, starch	9	5/0/2
Gly*, glu**, pyruvate	9	2/2/2
Purine, uracil	3	3/2/1
Purine, adenine	7	3/3/1
Purine, xanthine/inosine	4	2/1/0
Purine, cytidine	4	1/0/1
Purine, thymine	3	0/0/0
Glycerolipid	7	4/5/0
Carnitine	4	1/2/0
Essential fatty acid	7	5/1/0
Fatty acid metabolism	5	4/0/0
Bile acid	10	6/1/0
Fatty acid, dicarboxylate	5	0/2/0
Long chain fatty acid	19	3/4/0
Inositol	3	1/0/0
Medium chain fatty acid	3	1/1/0
Lysolipid	35	3/5/1
Sterol/steroid	6	0/1/0
Sphingolipid	4	0/0/0
Nicotinate, nicotinamide	3	3/0/1
Folate	5	0/3/0
Ascorbate and aldarate	3	1/0/0
Pantothenate and CoA	4	1/1/1
Riboflavin	3	0/0/0
Food component/plant	9	4/4/0
Krebs cycle	5	0/2/0

Fig. S2. Spectra for uridine and uracil and the number of rhythmic metabolites in WT and *Clock*-deficient livers. (*A*) Uridine and uracil spectra from livers alongside the spectra for purified standards. *x* axis = *m/z* and *y* axis = relative level of the compound identified. (*B*) Liver metabolites from WT and *Clock*-deficient animals were analyzed using JTK_CYCLE, a nonparametric statistical test used to detect cycling events. When a *P* of 0.05 is considered significant, 21 metabolites are rhythmic in *Clock*-deficient animals. Of these, 12 are also rhythmic in WT livers. When *P* values of $\leq$0.01 are considered significant, 39 metabolites are rhythmic in WT livers but only 7 metabolites are rhythmic in *Clock*-deficient livers. (*C*) Number of identified metabolites for each metabolic subpathway as well as the number of named biochemicals showing a time or genotype effect or a time/genotype interaction.

A

Statistical comparisons *significantly altered biochemicals*			
Two-way ANOVA	**Genotype main effect**	**Time main effect**	**Genotype:time interaction**
Total biochemicals $p \leq 0.05$	132	172	22
Named biochemicals $p \leq 0.05$	73	100	17

B

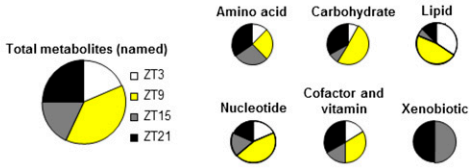

C

Clock-deficient vs. WT statistical comparisons *significantly altered biochemicals (named only)*				
ANOVA contrasts F-test	**ZT3**	**ZT9**	**ZT15**	**ZT21**
Total biochemicals $p<0.05$	**39**	**37**	**27**	**26**
Biochemicals (↑↓)	**18/21**	**20/17**	**14/13**	**8/8**

D

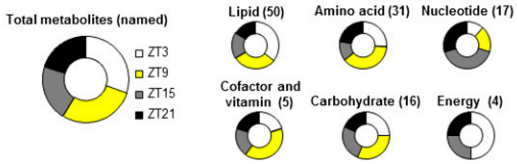

Fig. S3. Changing metabolite levels in wild-type and *Clock*-deficient livers at different zeitgeber times. (*A*) Number of total and named biochemicals in the liver showing a main effect of genotype or time or a genotype:time interaction. (*B*) Of 100 named metabolites identified as having a time main effect in the liver, the largest percentage of metabolite peaks occurred at the ZT9 time point (38%) followed by ZT21 (25%), ZT3 (19%), and ZT15 (18%). (*C*) Number of named biochemicals altered in the *Clock*$^{-/-}$ livers at a particular ZT and the distribution of up or down (↑↓) metabolites relative to WT livers. (*D*) Percent of total metabolites and metabolites within distinct subclasses identified as altered at a particular zeitgeber time in *Clock*$^{-/-}$ livers.

A

Metabolite	Time Effect?	Genotype Effect or Changed in *Clock* KO at a particular ZT time?	Genotype/Time Interaction?	Diurnal by JTK cycle in WT?	Diurnal by JTK cycle in KO?
Daidzein	Yes	Yes	No	No, p=0.087	Yes, p=0.036
Genistein	Yes	No	No	No	No
Equol	Yes	Yes	No	No	Yes, p=0.010
Stachydrine	Yes	Yes, ZT21	No	Yes, p=0.036	No
12-dehydrocholate	Yes	Yes, ZT9	No	Yes, p=0.017	No, p=0.087
Taurocholate	Yes	Yes, ZT3	No	Yes, p=0.010	No
6-beta-hydroxylithocholate	Yes	No	No	No	No
Beta-muricholate	Yes	No	No	Yes, p=0.017	No
Tauro-beta-muricholate	Yes	Yes, ZT3	Yes	Yes, p=0.00017	No

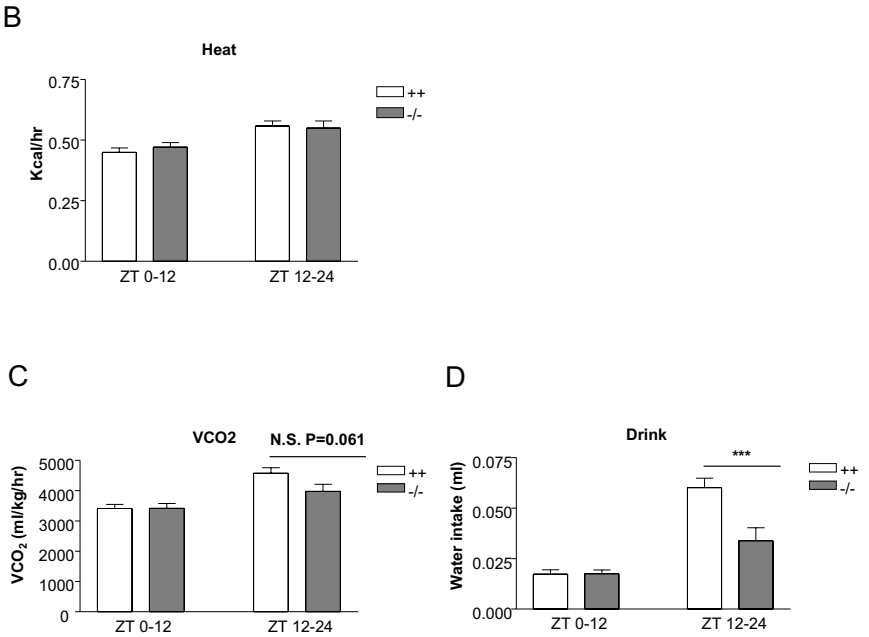

Fig. S4. Food-related and bile acid metabolite changes and additional metabolic characteristics of WT and *Clock*-deficient mice during night and day. (*A*) Food-related and bile acid metabolite changes showing a time or genotype effect or a time/genotype interaction. Rhythmicity of 24-h was determined for each metabolite by JTK_CYCLE. Heat (*B*) of WT and *Clock*-deficient animals was calculated by Oxymax software based on the VO_2 and respiratory exchange ratio (RER) measurements (*Methods*). VCO_2 and water intake (*C* and *D*) were measured over the 24-h cycle via indirect calorimetry. n = 7–8 animals per genotype.

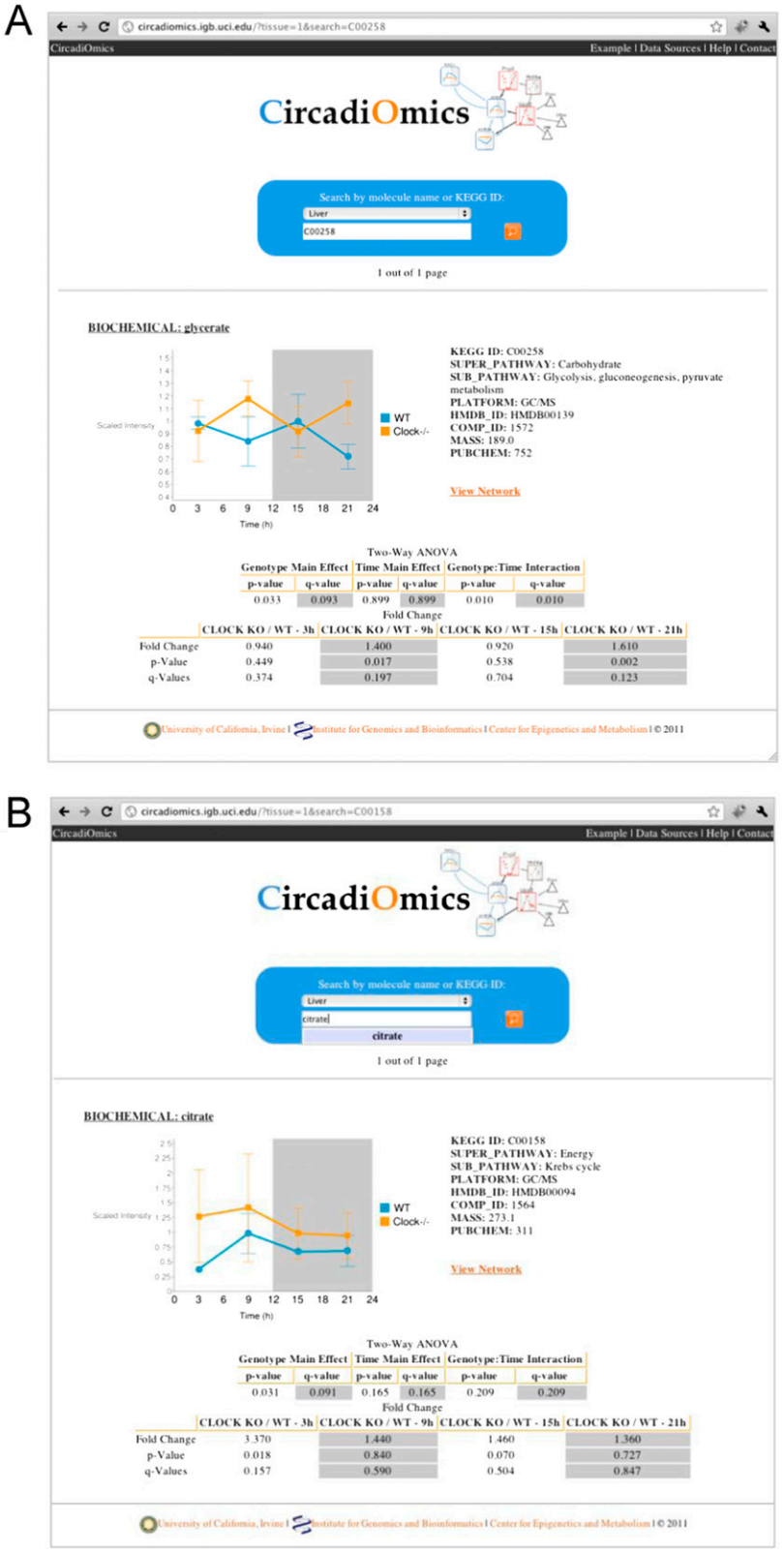

Fig. S5. The database CircadiOmics depicts the circadian properties and interactions of liver metabolites in WT and *Clock*-deficient livers. Screenshots from the CircadiOmics Webserver show search results of the terms "glycerate" (*A*) and "citrate" (*B*). CircadiOmics is a database that allows users to search for a metabolite and find relevant information concerning its expression in WT and *Clock*-deficient livers throughout the circadian cycle. Molecules can be searched for using the metabolite name or the KEGG ID. Once found, two-way ANOVA results can be observed for the metabolite as well as the statistical value attained in comparing metabolite abundance in *Clock*-deficient vs. WT livers at a given zeitgeber time. All genes in the network link to UniProt by double clicking, and the compounds link to KEGG.

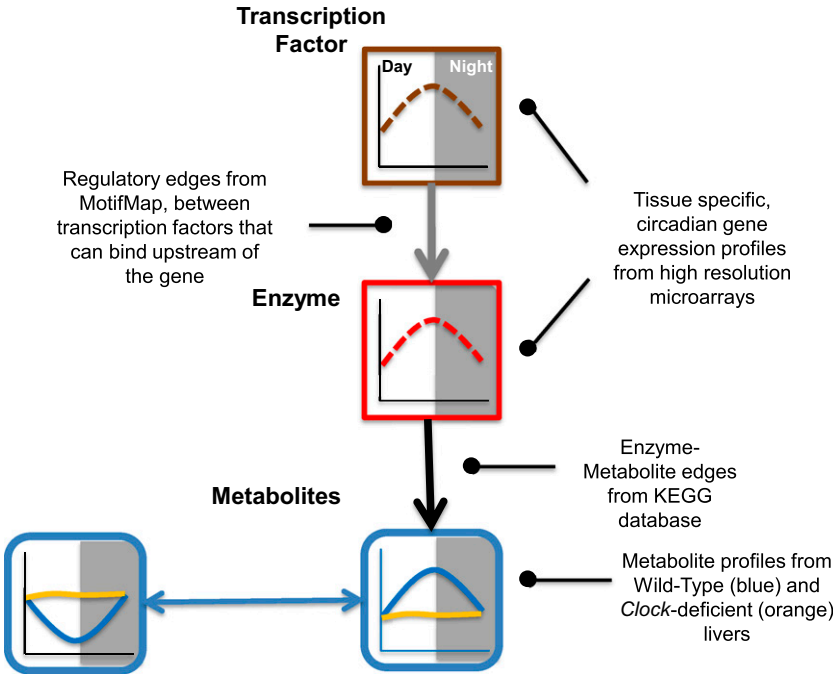

Fig. S6. Metabolite networks predict interactions between circadian gene expression and metabolism. Flowchart depicts assembly of CircadiOmics metabolite nodes. Data from CIRCA gene expression studies, GEO, MINT, BioGRID1, InAct, KEGG, MotifMap, and hepatocyte Bmal1 ChIP-seq experiments were used to build predicted metabolic nodes.

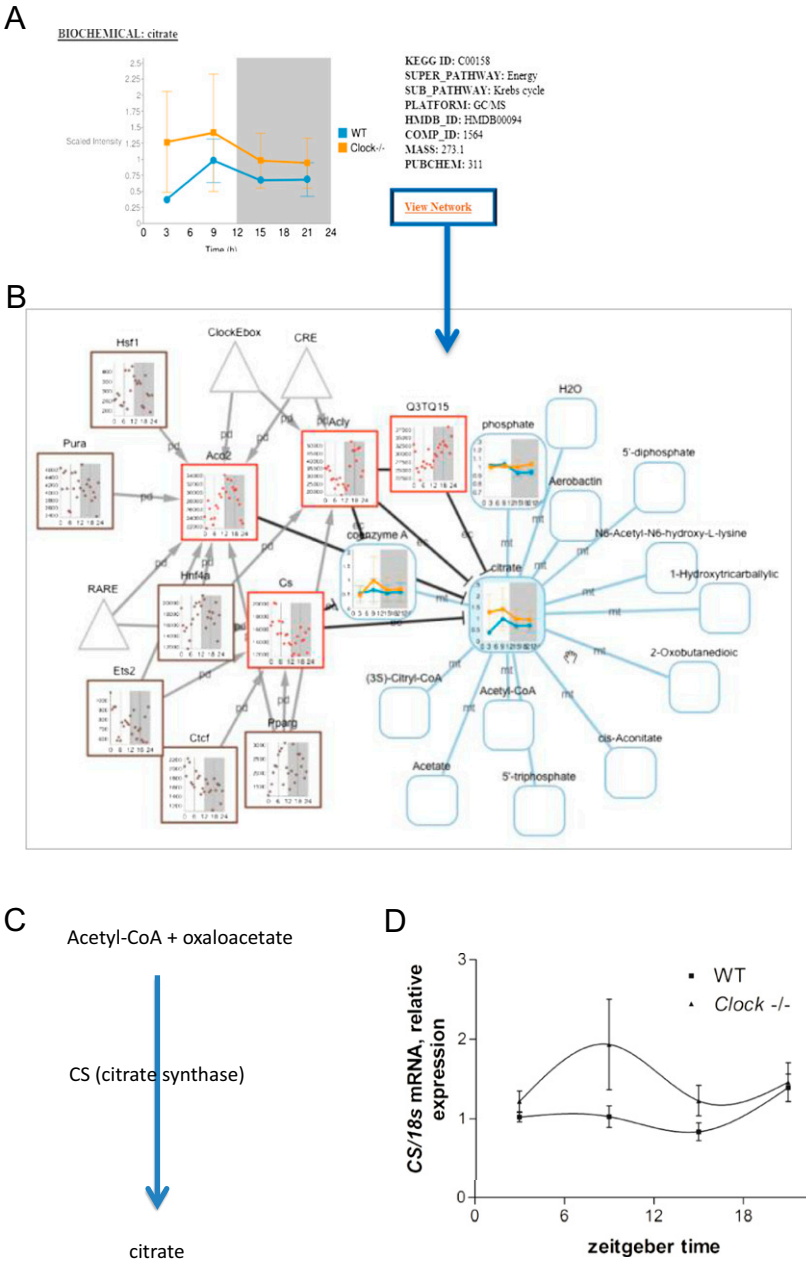

Fig. S7. The citrate node reflects regulation by clock in the liver. Although not rhythmic in WT animals, citrate was elevated in *Clock*-deficient livers (*A*) and mapping reveals the contribution of several enzymes, including citrate synthase (CS) and ATP citrate lyase (ACLY), to citrate levels in the cell (*B*). Citrate synthase contributes to the production of citrate via a reaction involving acetyl-CoA and oxaloacetate (*C*). (*D*) CS mRNA is elevated in *Clock*$^{-/-}$ livers, particularly at ZT15 (genotype main effect, $P < 0.05$, two-way ANOVA; $n = 5$ per time point per genotype).

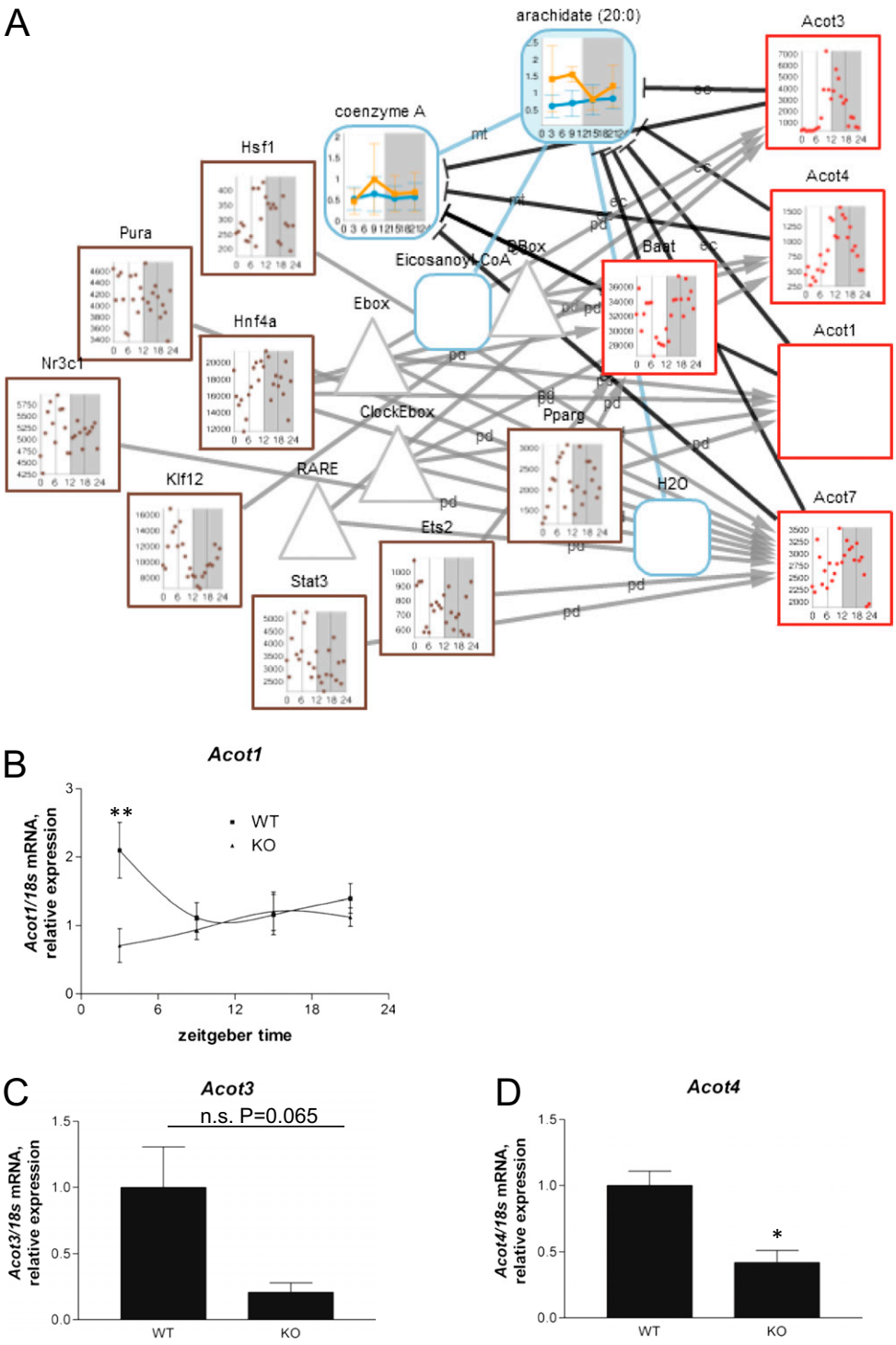

Fig. S8. Arachidate (C20:0) is elevated in *Clock*$^{-/-}$ livers. The arachidate node reveals the contribution of several acyl-CoA thioesterase enzymes to arachidate homeostasis (*A*). (*B*) *Acot1* mRNA was depressed in *Clock*$^{-/-}$ livers as analyzed by qPCR (time main effect, $P < 0.05$; genotype main effect, $P < 0.05$, two way ANOVA; $^{**}P < 0.01$, Bonferroni posttest). *Acot3* mRNA (*C*) and *Acot4* mRNA (*D*) were analyzed independently by microarray analysis in livers at ZT9. mRNAs for *Acot3* and *Acot4* were repressed in *Clock*-deficient livers ($^{*}P = 0.015$, unpaired *t* test; $n = 3$–5 livers per time point per genotype).

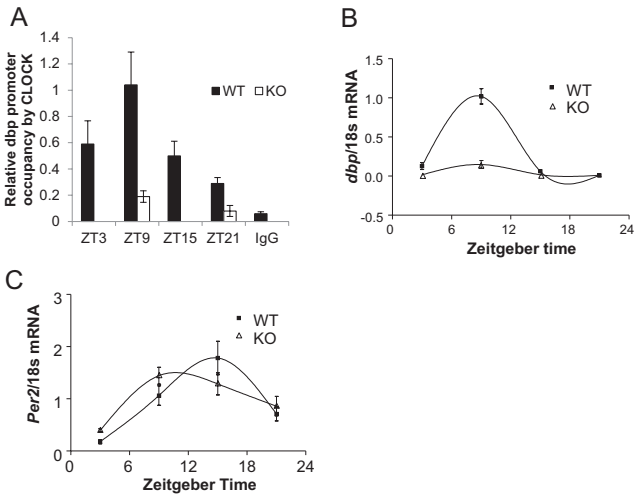

Fig. S9. Chromatin immunoprecipitation analysis of CLOCK binding to the *Dbp* promoter. Livers from WT and *Clock*$^{-/-}$ animals, were analyzed for Clock binding at target E boxes. Whereas CLOCK binding to target sites in the *Upp2* promoter showed a circadian profile of binding with a peak at ZT15 (Fig. 5), binding by CLOCK to the *Dbp* promoter in the same livers showed the expected circadian profile, with a peak in CLOCK binding at ZT9 (*A*). (*B*) *Dbp* mRNA expression in livers from WT and *Clock*$^{-/-}$ animals normalized to 18s (time main effect, $P < 0.0001$; genotype main effect, $P < 0.0001$, two way ANOVA. $n = 5$ per genotype per time point).

Dataset S1. Heat map of statistically significant biochemicals in WT and *Clock*-deficient mouse livers

Dataset S1 (XLSX)

Heat map metabolites are grouped according to their metabolic pathway and subpathway. Cells containing numerical fold change values show the relative abundance of the metabolite in the *Clock*-deficient liver divided by the relative abundance of the metabolite in WT liver at that same zeitgeber time (ZT3, ZT9, ZT15, and ZT21). Red shading within cells indicates that the mean values are significantly higher for the comparison, whereas green shading demonstrates a significantly lower value. All red and green shaded cells meet significance. Fold change numbers that are in blue and bold font have a P value of <0.10. Blue shaded cells indicate which metabolites show a main effect of time, a main effect of genotype, or a time:genotype interaction ($P < 0.05$, two-way ANOVA).

Dataset S2. Metabolites with circadian periodicity in WT livers as analyzed by JTK_CYCLE

Dataset S2 (XLSX)

Metabolite expression profiles were analyzed using a nonparametric algorithm (JTK_CYCLE) to determine whether circadian periodicity could be detected. Data are organized according to the adjusted P value for all WT metabolites identified in the study.

Dataset S3. Metabolites with circadian periodicity in *Clock*-deficient livers as analyzed by JTK_CYCLE

Dataset S3 (XLSX)

Metabolite expression profiles were analyzed using a nonparametric algorithm (JTK_CYCLE) to determine whether circadian periodicity could be detected. Data are organized according to the adjusted P value for all metabolites identified in the study for *Clock*-deficient livers.

Dataset S4. JTK_CYCLE and ANOVA analysis for all identified metabolites

Dataset S4 (XLSX)

JTK_CYCLE and ANOVA P and q values for all metabolites as well as permutation test scores.